

## Heavy-ion transfer reactions as a diffusion process

H. Oeschler, J. P. Coffin, P. Engelstein, A. Gallmann, K. S. Sim, and P. Wagner

*Centre de Recherches Nucléaires et Université Louis Pasteur, 67037 Strasbourg Cedex, France*

(Received 5 December 1977)

The transfer reactions induced by  $^{28}\text{Si}$  on  $^{130}\text{Te}$  at  $E_{\text{lab}} = 140$  MeV exhibit properties which can be explained with the picture of classical Coulomb trajectories (angular distributions, limited mass transfer, average  $Q$  values). However, several characteristics such as strongly decreasing average  $Q$  values at forward angles can be understood only in terms of multiple interactions. Presentation of the data as a function of angle, energy loss, and transferred mass reveals the two aspects: the domain of one-step character and the region of multistep processes. Applying a diffusion model, the mass and energy transport coefficients are deduced. They agree well with those obtained from deep inelastic collisions.

NUCLEAR REACTIONS  $^{28}\text{Si} + ^{130}\text{Te}$ ;  $E = 140$  MeV; transfer reactions; measured  $\langle Q \rangle$  and  $\langle \Delta A \rangle$ ; deduced drift and diffusion coefficients for energy dissipation and mass transport.

### I. INTRODUCTION

Since heavy-ion beams have become available, several studies have dealt with gross properties of heavy-ion induced transfer reactions above the barrier.<sup>1-4</sup> Due to the strong Coulomb repulsion between the nuclei on one hand, and the strength of the absorption at small impact parameters on the other, only a rather limited range of impact parameters can contribute to these reactions. The large Sommerfeld parameter  $\eta$  justifies in most of the cases the picture of classical trajectories leading to bell-shaped angular distributions. The most probable  $Q$  values can be explained in this picture too. Even details like the angular dependence of the average  $Q$  values can be described by taking into account the exact geometry of the trajectories.<sup>5</sup>

The reaction  $^{28}\text{Si}$  on  $^{130}\text{Te}$  ( $\eta = 51$ ) seems to follow this simple picture. Nevertheless, several observations are in conflict with this idea and the aim of this article is to show two aspects of quasielastic reactions, one which agrees with the known classical behavior and one which indicates a different mechanism. At higher energies or between very heavy partners, new phenomena like deep inelastic collisions arise. The  $^{28}\text{Si}$  on  $^{130}\text{Te}$  reaction already exhibits at a rather low energy ( $E/V_C = 1.2$ ) the connection between the two domains.

### II. EXPERIMENTAL TECHNIQUE

A  $^{28}\text{Si}$  beam of 140 MeV was delivered by the up-graded Strasbourg MP tandem equipped with double-foil stripper. The target consisted of a  $200 \mu\text{g}/\text{cm}^2$  layer of enriched  $^{130}\text{Te}$  (99.5%) evaporated onto a  $15 \mu\text{g}/\text{cm}^2$  carbon backing. The light

reaction products were identified by a time-of-flight setup. At 50 cm from the target, the particles traversed a  $10 \mu\text{g}/\text{cm}^2$  thick carbon foil inclined at  $45^\circ$  and the emerging secondary electrons were focused onto a double channel plate (chevron assembly) to give a fast start signal. After a flight path of 108 cm, the particles were stopped in a solid-state detector, which provided a stop signal and energy information. A time resolution of 250 ps was obtained under beam conditions. No separation for the different  $Z$  was provided as the  $Q$  values allow in nearly all cases a distinction between the isobars and for most of the conclusions the  $Z$  information is not needed. Figure 1 shows on the left side a two-dimensional energy-mass spectrum. On the right, three energy spectra of mass 27 demonstrate the variation of the shape with angle (this effect will be discussed in Sec. III B). Relative normalization was done to the dead-time corrected counting rates of two monitor counters situated at  $28^\circ$  left and right of the beam axis. Absolute values to an accuracy of 5% were obtained by normalizing to elastic scattering at forward angles. The closely lying individual states in the final nuclei were not resolved and the low-lying inelastic excitations were not separated from the elastic scattering.

### III. RESULTS AND DISCUSSION

The angular distributions of the elastic scattering and the transfer reactions of  $^{28}\text{Si}$  on  $^{130}\text{Te}$ , as displayed in Fig. 2, show the usual behavior. The Fresnel-type elastic scattering can be well fitted with a Woods-Saxon potential. The solid curve represents the results of the optical-model code GENOA<sup>6</sup> with the following set of parameters:

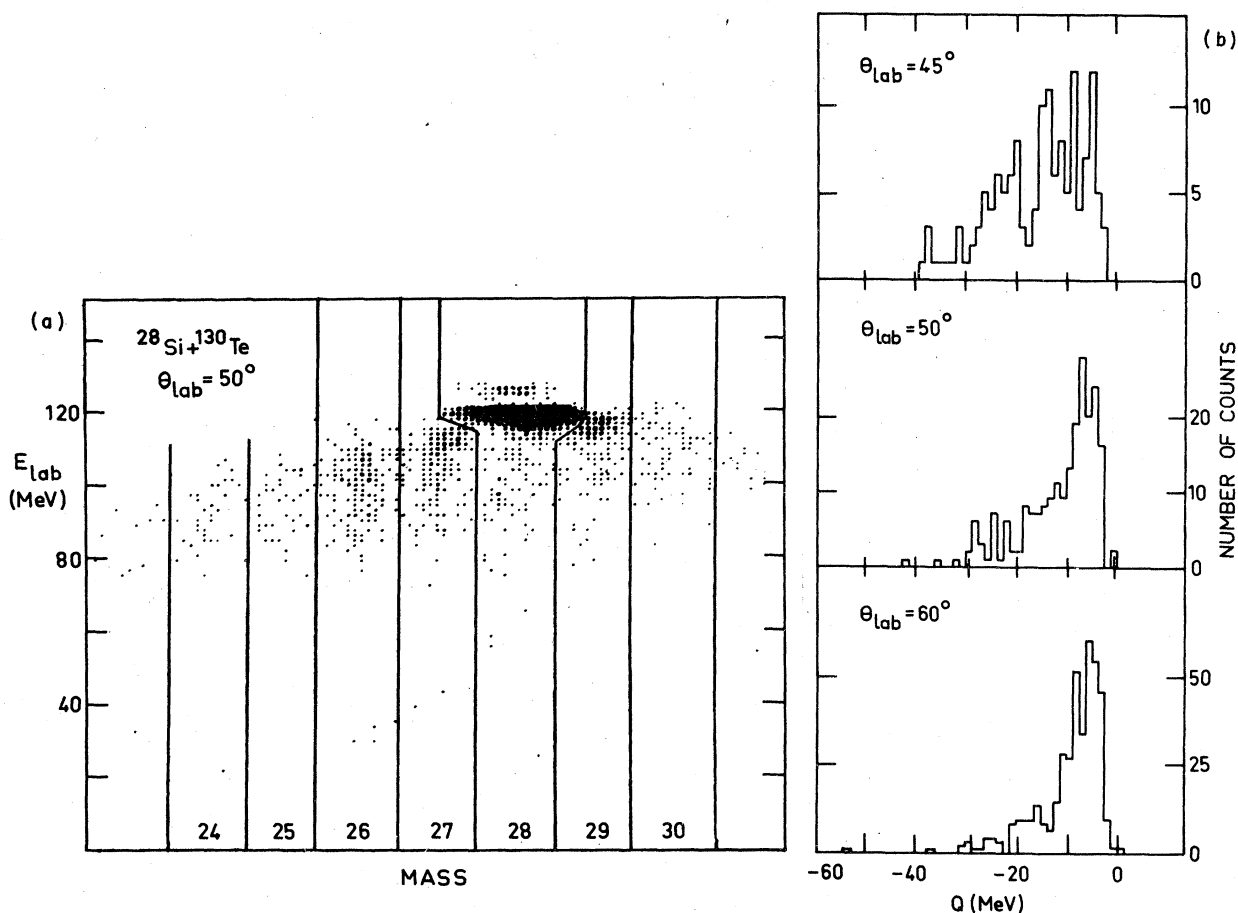


FIG. 1. (a) Two-dimensional spectrum of the reaction  $^{28}\text{Si}$  on  $^{130}\text{Te}$  showing that the cross section of the quasielastic processes is concentrated in the transfer of a few nucleons and a limited energy loss. Polygons set with the computer are separating the masses. (b) The energy spectrum of mass 27 at several angles exhibits the broadening at the forward angles.

$V = 54$  MeV,  $r_r = 1.212$  fm,  $a_r = 0.52$  fm,  $W_v = 25$  MeV,  $r_i = 1.362$  fm, and  $a_i = 0.3$  fm.

The sum of all transfer channels (crosses and thick line in Fig. 2) exhibits a bell-shaped angular distribution with the maximum (at  $63^\circ$ ) close to the rainbow angle (at  $61^\circ$ ). The individual mass-transfer channels show similar distributions with maxima varying slightly in angle because of the differing Coulomb forces in the exit channels.

The magnitude of the cross sections for the different channels decreases with increasing mass transfer. Not more than four nucleons are transferred in the stripping reactions, and in the pickup reactions only the transfer of one and two neutrons is observed.

It can be assumed that the reaction products have the same temperature and therefore the excitation energy is divided according to the mass; i.e., it is nearly completely taken by the heavy

partner.<sup>7</sup> Therefore, a possible particle decay of the light product can be excluded.

#### A. Average $Q$ values

The observed average  $Q$  values at the maxima of the angular distributions are compared with predictions in Table I. The indicated  $Z$  values result from comparison between ground-state  $Q$  values, optimum  $Q$  values ( $Q_{\text{opt}}$ ), and the experimental observations. The experimental  $\langle Q \rangle$  values of all the exit channels are lower than the predictions by the relation for continuous Coulomb trajectories<sup>1,2</sup>

$$Q_{\text{opt}} = E_{\text{c.m.}}^t \left( \frac{z_f Z_f}{z_i Z_i} - 1 \right),$$

where  $E_{\text{c.m.}}^t$  denotes the c.m. energy,  $z$  and  $Z$  the charges in the entrance ( $i$ ) and exit ( $f$ ) channels, respectively. A more refined formula<sup>5</sup> which

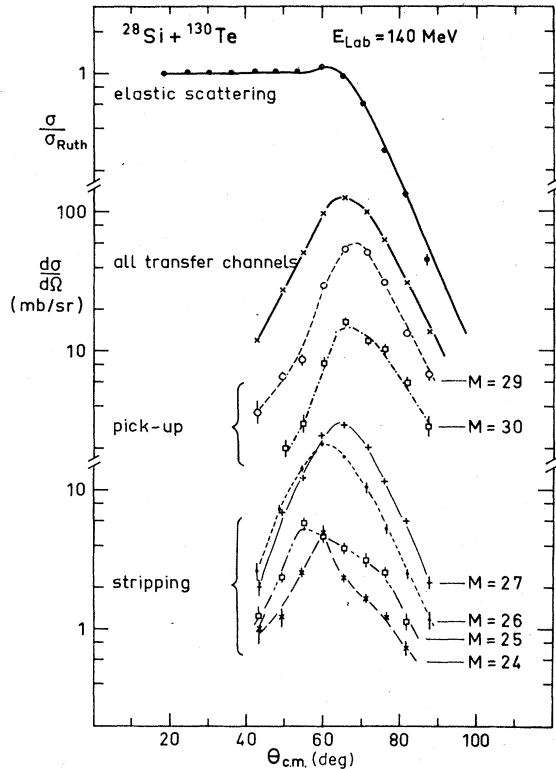


FIG. 2. Angular distributions of the elastic and quasi-elastic reactions of  $^{28}\text{Si}$  on  $^{130}\text{Te}$ . An optical model fit to the elastic scattering is represented as the thick line in the upper part of the figure. The curves through the data points of the transfer reactions are to guide the eye. The stripping reactions are displaced by one decade in the cross section. Statistical uncertainties are given whenever they exceed point size.

takes the displacement at the instant of interaction into account gives

$$Q_{\text{opt}}(\theta_i) = E_i \left\{ \frac{2}{1 + \csc(\theta_i/2)} \left[ \left( \frac{z_i Z_f}{z_i Z_i} \right) \alpha - \beta \right] + \beta - 1 \right\},$$

where  $\alpha$  and  $\beta$  (defined in Ref. 5) contain the shift

in the centers of gravity. The angular dependence will be discussed later on. This formula gives lower  $Q_{\text{opt}}$  values than the simple  $Q_{\text{opt}}$  formula at the maxima of the angular distributions, but the experimental quantities are still lower. The different values for the Mg isotopes resulting from the formula are in the same sequence as found in the experiment.

The excitation energy of the Mg isotopes is highest for the largest number of transferred nucleons. A similar observation is made for the Si isotopes which are reached by pickup reactions. We eliminate the possibility that a considerable number of the events with mass 30 originate from the ( $^{28}\text{Si}$ ,  $^{30}\text{P}$ ) reaction which has a  $Q_{\text{g.s.}}$  of  $-3.9$  MeV because the observed  $Q$  values start at higher values and show no threshold, and because the cross section of mass 30 amounts to 30% of that of mass 29. This would be far too high for such a badly matched reaction. Two possible explanations will be discussed in the following paragraphs. The first is in the frame work of direct processes; the second is in terms of deep inelastic collisions.

It is highly probable that the multi-nucleon-transfer reactions take place at smaller distances than the one-nucleon transfers. This causes lower  $\langle Q \rangle$  values if the other matching conditions are equal, and this may be the reason why the  $\langle Q \rangle$  values of the outgoing Si and Mg isotopes are decreasing with increasing number of transferred nucleons.

The other interpretation concerns the energy balance. The total amount of energy which can be converted into internal excitation ( $E_{\text{avail}}^{\text{out}}$  in Table I) is the energy above the barrier in the exit channel plus the difference in the binding energies. For grazing collisions, a large fraction of this available energy is energy of relative rotation, which can only be converted into internal excitation by tangential friction. If we assume the reaction to be fully relaxed in the radial degree of freedom and only partly in the tangential one, the

TABLE I. Summary of predicted and experimental  $Q$  values and related quantities (all values are given in MeV).

Outgoing particle		Predicted values			$E_{\text{avail}}^{\text{out}}$	$\langle Q \rangle_{\text{at } \theta_{\text{max}}}^{\text{exp.}}$	$\langle E_x \rangle_{\text{at } \theta_{\text{max}}}^{\text{exp.}}$	$\frac{E_{\text{avail}}^{\text{out}} - \langle E_x \rangle^{\text{exp.}}}{E_{\text{avail}}^{\text{in}}}$
A	Z	$Q_{\text{opt}}^{\text{a}}$	$Q_{\theta=65}^{\text{b}}$	$Q_{\text{g.s.}}$				
30	14	0	+7.7	+4.58	34.0	-4.5	9.1	0.86
29	14	0	+3.7	+0.09	29.3	-3.3	3.4	0.90
27	13	-6.2	-8.0	-4.19	29.1	-9.6	5.4	0.82
26	12	-12.7	-15.6	-3.34	34.6	-17.0	13.7	0.73
25	12		-18.3	-7.91	29.8	-22.4	14.5	0.53
24	12		-20.7	-6.78	30.7	-23.8	17.0	0.47

<sup>a</sup>References 1 and 2.

<sup>b</sup>Reference 5.

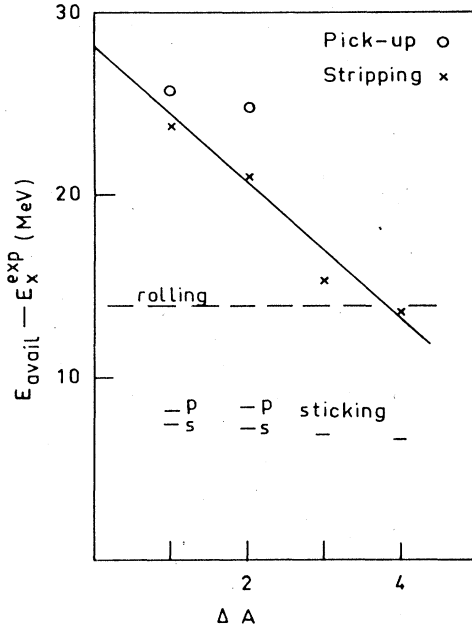


FIG. 3. The energy of relative rotation in the exit channel ( $E_{\text{avail}} - \langle E_x \rangle^{\text{exp}}$ ) vs transferred mass  $\Delta A$ . The limit of tangential friction for several configurations are shown: rolling condition as the dashed line and sticking condition as horizontal bars (p and s refer to pickup and stripping). No more than four nucleons are transferred and this limit coincides with the rolling condition.

value  $E_{\text{avail}}^{\text{out}}$  minus the experimental excitation energy represents the remaining energy of relative rotation in the exit channel.

In Fig. 3 this value is plotted vs the transferred mass  $\Delta A$ . The energy of relative rotation decreases by about 3.6 MeV or 13% per transferred nucleon. The trend in the pickup processes is very similar, and it can be seen that the gain from the binding energies in the  $^{30}\text{Si}$  exit channel of +4.5 MeV is fully converted into internal excitation. The one-neutron pickup to  $^{29}\text{Si}$  has a  $Q_{\text{g.s.}}$  of approximately zero.

In Fig. 3 the limits of the relaxation in the tangential mode are also indicated. In the case of a rigid connection between the nuclei (sticking condition) the ratio between the relative angular momenta is given by

$$l_f/l_i = \mathcal{G}_{\text{rel.}} / (\mathcal{G}_{\text{rel.}} + \mathcal{G}_1 + \mathcal{G}_2),$$

where  $l_i$  and  $l_f$  are angular momenta in the entrance and exit channels, respectively.  $\mathcal{G}_{\text{rel.}}$  represents the relative moment of inertia ( $\mu R^2$ ), and  $\mathcal{G}_1$  and  $\mathcal{G}_2$  the internal ones. In a rolling condition  $l_f/l_i$  equals  $\frac{5}{7}$  and consequently,  $E_f^{\text{rel.rot.}} = (\frac{5}{7})^2 E_i^{\text{rel.rot.}}$ . As  $E_i^{\text{rel.rot.}}$  is taken from elastic scattering, the final energies are calculated on the basis of the grazing angular momentum. It is in-

teresting to note that experimentally, only up to four nucleons are transferred and this limit coincides with the rolling condition.

Whether the arguments of complete relaxation in the radial degree of freedom and a partial relaxation of the tangential motion are appropriate must be examined with other transfer reactions at low energies with well chosen ground-state  $Q$  values. For multi-nucleon-transfer reactions well above the barrier, where one expects deep inelastic collisions, similar arguments gave a consistent picture.<sup>7</sup>

### B. Diffusion-model analysis

Studying the angular dependence of the  $\langle Q \rangle$  values may give some insight into the mechanism. For example, the correct treatment of the concept of classical trajectories shows that the contributions vary with angle.<sup>5</sup> At very backward angles and at much higher energies, the decreasing  $Q$  values are also interpreted as being due to the influence of radial friction.<sup>8</sup> For angles around the grazing angle and for larger angles, the observed tendency is reproduced by the classical formula as shown in Fig. 4(a). The strongly decreasing  $Q$  values at forward angles both for the stripping and the pickup reactions mark a clear deviation from the assumption of classical nondissipative trajectories. Only minor deviations could be explained by taking the nuclear attraction into account in the deflection function. Distorted-wave Born-approximation (DWBA) calculations<sup>9</sup> for this reaction using an average form factor<sup>4</sup> exhibit  $\langle Q \rangle$  values decreasing with increasing angle. This trend has also been reported in Ref. 10 and is similar to the semiclassical results. Yet the absolute values obtained by these calculations are very sensitive to the strength functions, which are unknown at present. The  $\langle Q \rangle$  values do not seem to be influenced by the transferred angular momentum.<sup>11</sup>

An explanation for the strongly decreasing  $\langle Q \rangle$  values at the forward angles may easily be seen from Fig. 4(b). The contour plot of the double differential cross section vs c.m. energy and c.m. angle shows the maximum of the cross section around the grazing angle with some extension to backward and forward angles. In addition, a fraction of the cross section follows a line from the maximum to forward angles and to smaller kinetic energies. The similarity with deep inelastic reactions is evident and we interpret this part as the onset of strong friction.<sup>12</sup> A part of the reaction proceeds via multiple interactions corresponding to a longer contact time. As the two nuclei rotate together, the ejectile is bent to forward angles and a larger fraction of kinetic energy above the barrier

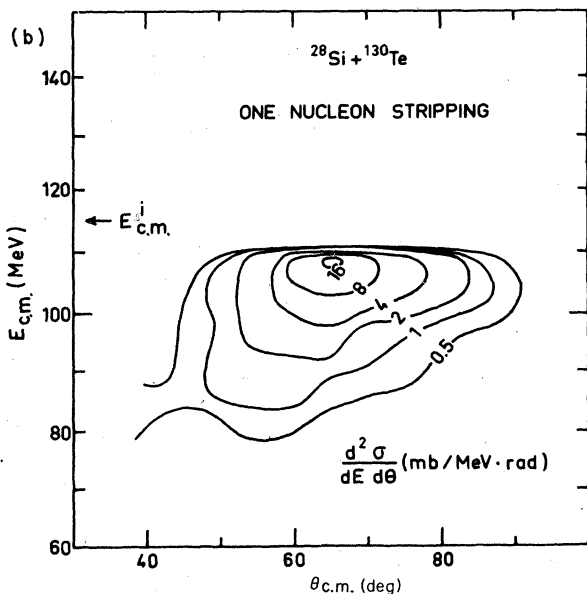
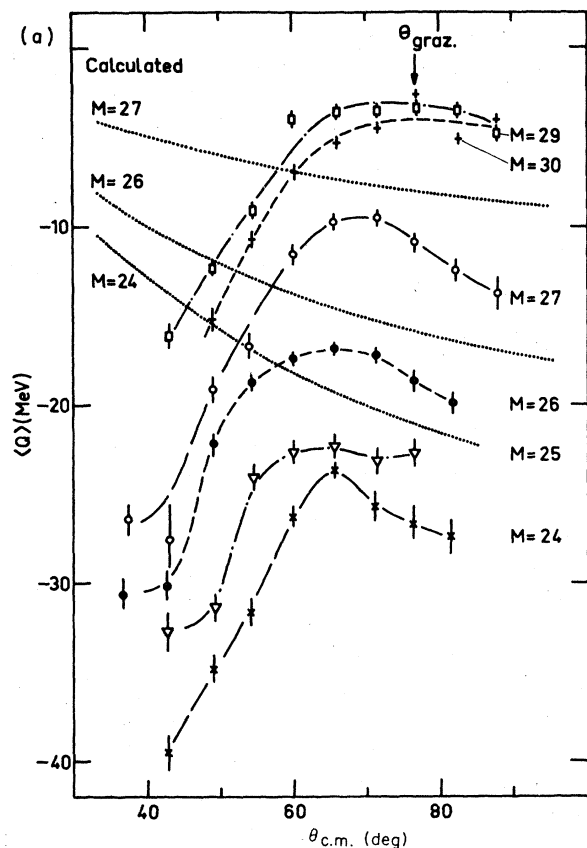


FIG. 4. (a) Experimental  $\langle Q \rangle$  values vs c.m. angle for all the transfer reactions. The pointed lines represent calculations based on the matching of Coulomb trajectories including "recoil effect" (Ref. 5). (b) Contour plot of the one-nucleon transfer.

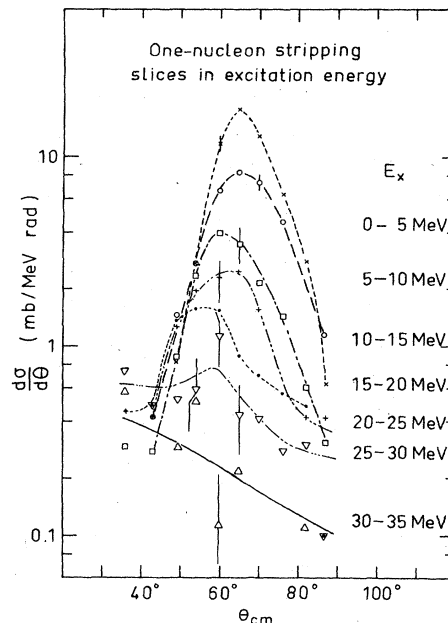


FIG. 5. Variation of the angular distributions for different windows in the excitation energy showing the evolution to the multistep interactions.

is converted into internal excitation. This interpretation can also be seen from Fig. 5 where the variation of the angular distributions for different slices in the excitation energy demonstrates the evolution to multistep processes. For the smallest excitation energies the usual bell-shaped angular distributions are obtained. With higher excitation energies the distributions broaden and the maxima are shifted to forward angles. Finally, one reaches rather flat distributions with a slight forward peaking at the highest excitation energies. This forward peaking is known from experimental and theoretical studies, done mostly for individual states, to be due to multistep processes.<sup>13</sup> Similar observations are made in the transfer reactions induced by  $^{16}\text{O}$  on Ca isotopes.<sup>14</sup> There this variation of the angular distributions is also shown as a function of the number of transferred nucleons. Yet one has to remember that these studies were made at higher energies ( $E/V_C = 1.4$ ) where one can expect multistep processes to take place.<sup>15</sup>

As there is evidence for multiple interactions, we applied a diffusion model to analyze the transfer reactions. The characteristic broadening of the  $Q$  value distribution as a function of angle and energy loss for the one-nucleon stripping reaction had been studied in a recent letter.<sup>12</sup> In the simple assumption of two nuclei rotating together, the deflection angle serves as a time scale.<sup>16</sup> Figures 6(a) and 6(b) show the experimental variance of

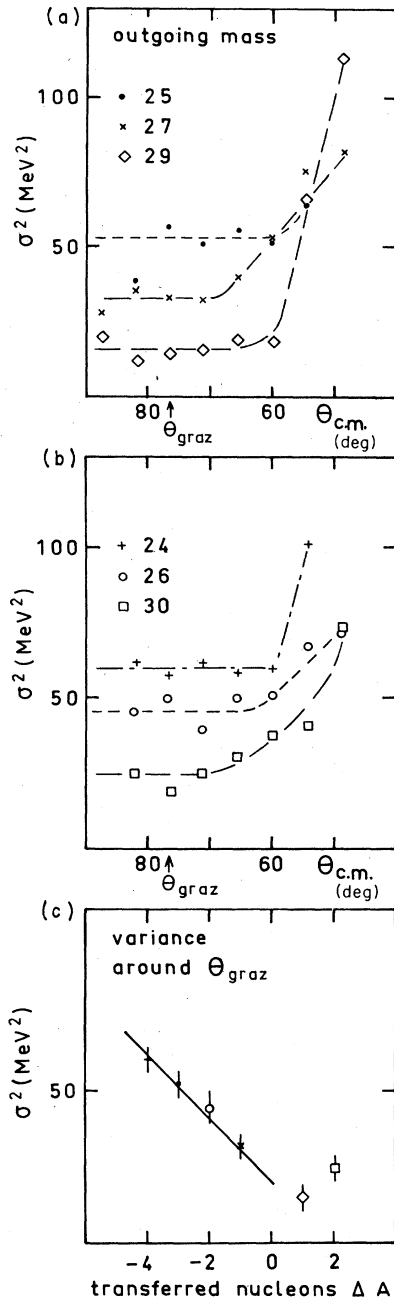


FIG. 6. (a), (b) Dependence of the variance in the energy distribution on the deflection angle for all the exit channels. (c) The values of the variance obtained around  $\theta_{\text{graz}}$ . vs the transferred mass  $\Delta A$ .

the energy distribution for all the transfer reactions. The trend of the one-particle stripping reaction [crosses in Fig. 6(a) and discussed in Ref. 12], a constant width around the grazing angle and for larger angles, and an increasing width at the forward angles, is seen for all cases. It shows

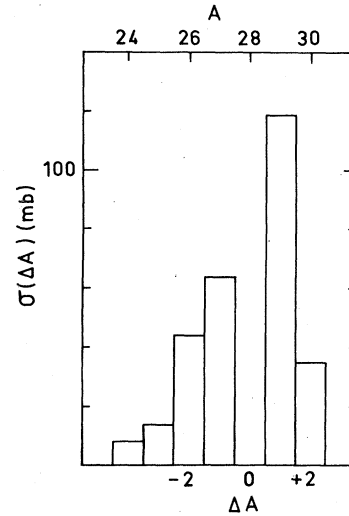


FIG. 7. Cross sections for the various mass transfer channels. The distribution is characterized by a smooth envelope.

again the two regimes, the “one-step character” around  $\theta_{\text{graz}}$ , and the “diffusion” at forward angles. A possible contribution from particle evaporation can be ruled out as already mentioned. This is emphasized by the observation of the same behavior in the pickup reactions. Using the Fokker-Planck equation with time-independent coefficients,<sup>16</sup> the values extracted from the one-nucleon transfer are for the diffusion coefficient<sup>12</sup>

$$D_E = 2.9 \times 10^{23} \text{ MeV}^2 \text{ s}^{-1}.$$

The diffusion coefficient was corrected for quantum fluctuations.<sup>12,17</sup> The slightly different slope in  $\sigma_E^2$  vs  $\theta_{\text{c.m.}}$  [Figs. 6(a) and 6(b)] at forward angles are not considered in the following.

The variance observed around the grazing angle, as displayed in Fig. 6(c) is quite different for the several channels and is strongly increasing as a function of  $\Delta A$ . It has been stated<sup>11</sup> that the width of the “Q window” depends on the transferred angular momentum, or, more precisely, on the shell-model state used in the form factor. As in all the transfer channels, a complicated mixture of different form factors “contribute”; it is not evident how this varies with the number of transferred nucleons. Yet this effect seems not sufficient to explain the slope.

The next point concerns the distribution of the cross section among the individual transfer channels, which is shown in Fig. 7. It is characterized by a smooth envelope as commonly seen in deep inelastic reactions.

In order to study the diffusion in the mass transfer, the angle is no longer a good time scale,

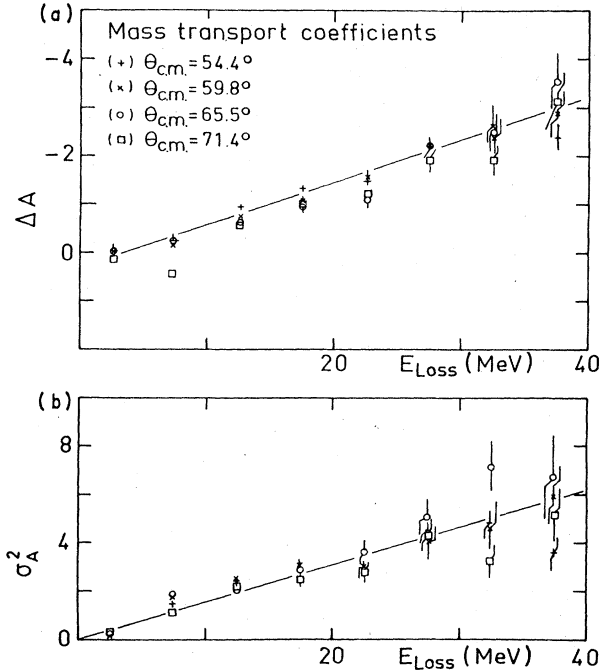


FIG. 8. (a) Transferred mass  $\Delta A$  vs energy loss. (b) Variance in mass vs energy loss.

since the different Coulomb fields in the exit channels shift outgoing particles with the same impact parameter to different angles. Therefore we have chosen the energy loss as a time scale. For several angles the mean value  $\Delta A$  and the variances  $\sigma_A^2$  as a function of energy loss are shown in Fig. 8. The results extracted at different angles coincide nicely. The values for elastic scattering mark the origin in the two figures and lie on the line through the experimental points, in agreement with the model of a simple diffusion mechanism. These two figures represent the mass drift coefficient  $v_A \cdot t$  versus  $v_E \cdot t$ , and the mass diffusion coefficient  $D_A \cdot t$  versus  $v_E \cdot t$ , respectively. Using the energy drift coefficient, we obtain a mass drift of

$$v_A = -2.4 \times 10^{22} \text{ s}^{-1},$$

and a diffusion of

$$D_A = 2.1 \times 10^{22} \text{ s}^{-1}.$$

The observed shift to the many-nucleon stripping reactions with increasing energy loss is, of course, not at all restricted to a diffusion mechanism. Such behavior is expected from optimum  $Q$  value arguments too. But the two models are not exclusive and the fact that the results for different angles coincide indicates a difference from a pure one-step character. Preliminary studies<sup>9</sup>

using the code DWUCK and an average form factor<sup>4</sup> multiplied by the square root of the level density to calculate the equivalent double differential cross section with one-step character, show a stronger shift in  $\Delta A$  with increasing energy loss and the lines for different angles are displaced parallel. These calculations show bell-shaped angular distributions very similar to the experimental ones, but their maxima lie close to the grazing angle, whereas the experimental curves are shifted by more than  $10^\circ$  to forward angles. A similar observation was made by Baltz<sup>18</sup> for the reaction  $\text{Ar} + \text{Th}$ , using the optical-model parameters obtained from elastic scattering.

According to the Einstein relation,<sup>16</sup> the drift of the mass transport is dominated by the derivative of the contact potential<sup>15</sup>  $\partial U_1(A_1)/\partial A_1$ . The value obtained from the experiment has the same sign as the calculations, but indicates a steeper slope of the contact potential  $U_1$ . In respect to this discussion, the present simple diffusion analysis should not be overstressed as several effects are neglected.<sup>19</sup>

The diffusion constants can be related to a coupling strength  $\gamma$ , a mean energy loss per step  $\Delta$ , an excitation energy  $E_x$ , and geometrical factors  $\alpha$  and  $\beta$  to take into account phase-space arguments<sup>16,17</sup>

$$D_E = \gamma_E \Delta_E^2 \sqrt{\Delta_E} E_x^{1/4} \alpha,$$

$$D_A = \gamma_A \sqrt{\Delta_A} E_x^{1/4} \beta.$$

In order to have a complete comparison between the present reaction and a typical deep inelastic reaction, e.g.,  $^{40}\text{Ar} + ^{232}\text{Th}$  which had been analyzed by Nörenberg,<sup>16</sup> we assume the same mechanism for the energy loss and the mass transfer. This allows extraction of unique values for  $\gamma$  and  $\Delta$  from our data which are

$$\gamma = 2.5$$

and

$$\Delta = 3.6 \text{ MeV}.$$

These values can be compared to  $\gamma = 2.07$  and  $\Delta = 4.3 \text{ MeV}$  obtained for the reaction  $^{40}\text{Ar}$  on  $^{232}\text{Th}$ . The extracted coupling strengths  $\gamma$  for the two reactions agree nicely. Both reactions have been analyzed with the same simple assumption of a rotating dinuclear system. The rather high values for the mean energy loss per step  $\Delta$ , indicate that one has mainly radial friction. Thus the above mentioned assumption of  $\gamma_E = \gamma_A$  is doubtful. Yet we would like to stress the close similarity of the extracted values for the two reactions, the present transfer and the typical deep inelastic process.

In general, one could object to the use of the dif-

fusion model in the case of a reaction which proceeds by only a few steps. We are sure that this is a lower limit but we feel that the diffusion model is justified by the linearity observed in several figures (6 and 8), the fact that the lines pass through the origin, and by the magnitude of the extracted values.

#### IV. SUMMARY

The quasielastic reaction of  $^{28}\text{Si}$  on  $^{130}\text{Te}$  at 140 MeV incident energy shows some features which are similar to those observed in other light heavy-ion induced transfer reactions and others which are in contrast to these. We like to point out that no clear distinction between a "one-step region" and a "diffusion region" can be made demonstrating a continuous evolution. The onset of multiple interactions is seen in this reaction at a relatively low energy ( $E/V_c = 1.2$ ).

The most interesting effect is seen in the angular dependence of the observed  $Q$  values. While the decreasing  $Q$  values at the backward angles agree with a one-step character, the strongly de-

creasing values at the forward angles are interpreted as being due to the onset of strong friction and multiple interactions. They are accompanied by a broadening which suggests the application of a diffusion model. To circumvent the distortion due to the differing Coulomb fields in the exit channels, the coefficients for the mass transfer were extracted by using the energy loss as a time scale. The derived coefficients and the deduced coupling strength agree very well with ones extracted from the deep inelastic collision  $\text{Ar} + \text{Th}$ .

This paper presents an analysis in the framework of a diffusion model. A one-step-interaction model could probably explain several of the experimental results, but certainly not all. For example, the observed enhancement of the stripping reactions is a common feature of semiclassical optimum  $Q$  values, of DWBA calculations, and of the contact potential. These models are closely related (Coulomb force) even if they start from physically very different grounds. They are not necessarily contradictory (see e.g. Ref. 20), but complementary.

<sup>1</sup>P. R. Christensen, V. I. Manko, F. D. Becchetti, and R. J. Nickles, Nucl. Phys. **A207**, 33 (1973).

<sup>2</sup>P. J. A. Buttle and L. J. B. Goldfarb, Nucl. Phys. **A176**, 299 (1971).

<sup>3</sup>W. Henning, J. P. Schiffer, D. G. Kovar, S. Vigdor, B. Zeidman, Y. Eisen, and H. J. Körner, Phys. Lett. **58B**, 129 (1975).

<sup>4</sup>H. Oeschler, G. B. Hagemann, M. L. Halbert, and B. Herskind, Nucl. Phys. **A266**, 262 (1976).

<sup>5</sup>J. P. Schiffer, H. J. Körner, R. H. Siemssen, K. W. Jones, and A. Schwarzschild, Phys. Lett. **44B**, 47 (1973); N. Anantaraman, K. Katori and J. P. Schiffer, in Proceedings of the Symposium on Heavy-Ion Transfer Reactions, Argonne, 1973 [Argonne National Laboratory Informal Report No. PHY 1973B, 1973 (unpublished)], Vol. II, p. 413.

<sup>6</sup>Code GENOA by F. Perey, revised version by B. Nilsson, Niels Bohr Institute, Copenhagen.

<sup>7</sup>H. Kamitsubo, in Proceedings of the Symposium on Macroscopic Features of Heavy-Ion Collisions, Argonne, 1976 [Argonne National Laboratory Informal Report No. PHY-76-2 (unpublished)], Vol. I, p. 177.

<sup>8</sup>J. Wilczynski, K. Siwek-Wilczynska, J. S. Larsen, J. C. Acquardo, and P. R. Christensen, Nucl. Phys. **A244**, 147 (1975).

<sup>9</sup>H. Oeschler, J. P. Coffin, P. Engelstein, A. Gallmann, K. S. Sim, and P. Wagner, in *Proceedings of the XVI Winter School on Nuclear Physics*, Bielsko, Poland, Feb. 20-March 5, 1978 (unpublished); (unpublished).

<sup>10</sup>F. D. Becchetti, D. G. Kovar, B. G. Harvey, D. L.

Hendrie, H. Homeyer, J. Mahoney, W. von Oertzen, and N. K. Glendenning, Phys. Rev. C **9**, 1543 (1974).

<sup>11</sup>D. G. Kovar, in *Proceedings of the International Conference on Reactions between Complex Nuclei, Nashville Tennessee, 1974*, edited by R. L. Robinson, F. K. McGowan, J. B. Ball, and J. H. Hamilton (North-Holland, Amsterdam/American Elsevier, New York, 1974). Vol. I, p. 235.

<sup>12</sup>H. Oeschler, J. P. Coffin, P. Engelstein, A. Gallmann, K. S. Sim, and P. Wagner, Phys. Lett. **71B**, 63 (1977).

<sup>13</sup>For example, D. K. Scott, in *Proceedings of the International Conference on Nuclear Physics, Munich 1973*, edited by J. de Boer and H. J. Mang (American Elsevier, New York, 1973), Vol. II, p. 215.

<sup>14</sup>S. E. Vigdor, in Proceedings of the Symposium on Macroscopic Features of Heavy-Ion Collisions, Argonne, 1976. (See Ref. 7), Vol. I, p. 95.

<sup>15</sup>L. G. Moretto and R. Schmitt, J. Phys. **37**, C5-109 (1976).

<sup>16</sup>W. Nörenberg, Phys. Lett. **52B**, 289 (1974); J. Phys. **37**, C5-141 (1976).

<sup>17</sup>S. Ayik, B. Schürmann, and W. Nörenberg, Z. Phys. **A277**, 299 (1976); **A279**, 145 (1976).

<sup>18</sup>A. J. Baltz, Phys. Rev. Lett. **38**, 1197 (1977).

<sup>19</sup>G. Wolschin and W. Nörenberg, Z. Phys. **A284**, 209 (1978); S. Ayik, G. Wolschin and W. Nörenberg, Report No. MPIH-1977-V39 (unpublished).

<sup>20</sup>V. E. Bunakov, Yad. Fiz. **25**, 505, (1977) [Sov. J. Nucl. Phys. **25**, 271 (1977)].